THE JOURNAL OF BIOLOGICAL CHEMISTRY
Vol. 272, No. 3, Issue of January 17, pp. 1956–1964, 1997
Printed in U.S.A.

Palmitylation of the Vaccinia Virus 37-kDa Major Envelope Antigen

IDENTIFICATION OF A CONSERVED ACCEPTOR MOTIF AND BIOLOGICAL RELEVANCE*

(Received for publication, October 17, 1996)

Douglas W. Grosenbach, David O. Ulaeto‡, and Dennis E. Hruby§

From the Center for Gene Research and Biotechnology, Department of Microbiology, Oregon State University, Corvallis, Oregon 97331-3804

Computer-assisted alignment of known palmitylproteins was used to identify a potential peptide motif, TMDX_{1-12}*AAC*(C)*A* (TMD, transmembrane domain; *X*, any amino acid; C, cysteine acceptor residues; *A*, aliphatic residue) responsible for directing internal palmitylation of the vaccinia virus 37-kDa major envelope antigen, p37. Site-directed mutagenesis was used to confirm this motif as the site of modification and to produce a nonpalmitylated version of the p37 protein. Comparative phenotypic analysis of the wild-type and mutant p37 alleles confirmed that the p37 protein is involved in viral envelopment and egress, and suggested that attachment of the palmitate moiety was essential for correct intracellular targeting and protein function.

Palmitylation involves the dynamic (reversible) post-translational addition of a 16-carbon saturated fatty acyl moiety via thioester or ester linkage to cysteine, serine, or threonine residues. Protein palmitylation has been demonstrated to play a variety of roles *in vivo*. When the function of palmitylation can be established, it usually falls into one of three categories. (i) Palmitylation can "activate" a protein, usually by targeting the protein to a site where it carries out its function (1) (the protein is then "inactivated" by depalmitylation); (ii) palmitylation can mediate protein-protein interactions (2); or, as is most often the case, (iii) palmitylation mediates protein-membrane interactions (2).

There are many examples of cellular and viral palmitylproteins (for reviews see Refs. 2–7). In many cases the palmitate acceptor residues have been identified, but a sequence or structural motif specifying palmitylation of proteins remains elusive. Recently a thioesterase demonstrated to cleave the palmityl group from proteins has been purified and cloned, but the enzyme(s) responsible for the addition of palmitate to proteins has not been identified. In some cases, palmitylation of one protein is dispensable for function, while on closely related proteins it is absolutely necessary for function. For example, the hemagglutinin of influenza virus is palmitylated on conserved cysteine residues of its cytoplasmic tail. For the H1 subtype of influenza, a partial block on palmitylation resulted in attenuation, and mutants in which the hemagglutinin was not palmitylated were not viable (8). Surprisingly, the hemagglutinin of the H3 subtype does not require palmitylation for the production of infectious particles (9). A similar disparity is found among cellular palmitylproteins. Palmitylation of the Src family of tyrosine kinases targets them to caveolae (1), while palmitylation of caveolin (a normally palmitylated constituent of caveolae) is not necessary for targeting to that structure (10).

Vaccinia virus (VV)[1] is a member of the *Poxviridae*, a family of large, complex DNA viruses that replicate in the cytoplasm of infected cells (11). With the eradication of smallpox, the focus on VV biology momentarily faded, but it has been "rediscovered" as a versatile tool for molecular biologists. This has spurred recent efforts to characterize the virus. The 191-kilobase pair genome has been completely sequenced (12) and appears to encode nearly 200 gene products. Many are involved in nucleic acid metabolism, immune modulation, or serve some other non-structural function, and about 100 are structural proteins that are packaged with the virion. The infectious virion may exist in one of four forms; intracellular mature virus (IMV), intracellular enveloped virus (IEV), cell-associated enveloped virus (CEV), and extracellular enveloped virus (EEV). IMV is the simplest in structure, being composed of the core particle and a double-layered membrane derived from the intermediate compartment between the endoplasmic reticulum and the Golgi stacks (13). By a process that is still poorly understood, IMV particles are targeted to the *trans*-Golgi and subsequently enwrapped by a double membrane derived from it (14, 15) resulting in the production of IEV. Virions then migrate to the cell surface, where by fusion and loss of the outermost membrane, followed by release into the medium, EEV are produced. If the virions remain attached to the outer face of the plasma membrane, they are referred to as CEV. This process is

* This work was supported by Research Grant AI-21335 from the National Institutes of Health. The costs of publication of this article were defrayed in part by the payment of page charges. This article must therefore be hereby marked "*advertisement*" in accordance with 18 U.S.C. Section 1734 solely to indicate this fact.

‡ Present address: Detection Centre, CDBE, Porton Down, Salisbury, Wilts SP40JQ, United Kingdom.

§ To whom correspondence should be addressed. Tel.: 541-737-1849; Fax: 541-737-2440; E-mail: hrubyd@bcc.orst.edu.

[1] The abbreviations used are: VV, vaccinia virus; IMV, intracellular mature virus; IEV, intracellular enveloped virus; CEV, cell-associated enveloped virus; EEV, extracellular enveloped virus; p37, 37,000-dalton vaccinia envelope antigen; gp42, 42,000-dalton vaccinia glycoprotein; p7.5K, vaccinia early/late promoter to a 7,500-dalton protein of unknown function; TGN, *trans* Golgi network; MEM-E, Eagle's minimal essential medium; LG, L-glutamine; GS, gentamycin sulfate; FCS, fetal calf serum; HPI, hours post-infection; m.o.i., multiplicity of infection; [^{3}H]PA, [9,10-^{3}H]palmitic acid; [^{3}H]OA, [9,10-^{3}H]oleic acid; PBS, phosphate-buffered saline; RIPA, radioimmunoprecipitation assay buffer; α-p37, rabbit polyclonal antiserum to the 37,000-dalton vaccinia envelope antigen; α-gp42, monoclonal antibody to the 42,000-dalton vaccinia glycoprotein; p4a, the vaccinia major core protein; α-p4a, rabbit polyclonal antiserum to the vaccinia major core protein; TK, the vaccinia-encoded thymidine kinase; α-TK, rabbit polyclonal antiserum to the vaccinia thymidine kinase; HB, hypotonic buffer; NP, nuclear pellet; PNS, post-nuclear supernatant; P15, the resulting pellet of a 15,000 × *g* centrifugation of the cytoplasmic fraction of cells; P100, the resulting pellet of a 100,000 × *g* centrifugation of the cytoplasmic fraction of cells; S100, the soluble component of cells as determined by differential centrifugation subcellular fractionation; GαR-FITC, goat antibodies conjugated to fluoroscein isothiocyanate and directed against rabbit IgG; GαM-TRITC, goat antibodies conjugated to tetramethyl rhodamine isothiocyanate and directed against mouse IgG; PAGE, polyacrylamide gel electrophoresis.

mediated by numerous VV-encoded proteins (16–20), including p37 and a 42-kDa glycoprotein (gp42).

Acylation of VV polypeptides has been demonstrated to play a major role in the assembly of virions. At least four proteins are myristoylated on glycine of the amino-terminal motif, methionine-glycine-(any 3 amino acids)-serine/threonine. The most studied of these is the 25-kDa protein product of the L1R open reading frame (21). Expression of a nonmyristoylated L1R protein within infected cells rather than the normally acylated protein resulted in a one-log reduction in titer relative to wild-type virus. It has also been previously demonstrated that there are at least six palmitylproteins induced in VV-infected cells (22). They are all present in the membrane fraction of cells and when virion-associated, are present in the outer membrane fraction of CEV and EEV. Three remain unidentified, and the others are encoded by VV open reading frames A34R (23), B5R (18), and F13L (14, 24), which express a 21–26-kDa glycoprotein, gp42, and the object of this study, p37, respectively.

Inactivation of the parental genes for either p37 or gp42 proteins in the VV genome results in varying degrees of inhibition on the envelopment and release of enveloped virions. One such deletion mutant is vRB10 (16), a derivative of the IHD-J strain of vaccinia. In this mutant, 93% of the F13L open reading frame (encoding p37) has been replaced with the *gpt* gene under the control of the VV 7.5-kDa promoter (p7.5K). During the characterization of this recombinant, a striking biological defect was noted. While producing normal amounts of IMV, the production of enveloped virus was severely inhibited. Additionally, the virus was not able to efficiently spread (in tissue culture) from cell to cell. Most strains of VV produce visible plaques within 24 h after infection of a permissive cell monolayer, but vRB10 requires at least 4 days before minute plaques are visible. Clearly, p37 is a major contributor to the envelopment and release process.

p37 is a 372-amino acid polypeptide expressed at late times during infection and has a predicted mass of 41 kDa. In gels it has an apparent mass of 37 kDa, which has been attributed to modifications that alter its electrophoretic mobility. Within infected cells, p37 localizes to the *trans*-Golgi network (TGN; Ref. 15) where it is tightly associated with the outer face of the organelle. The significance of the palmitate moiety in mediating membrane attachment has been demonstrated *in vitro* (25), and we sought to confirm and extend that work *in vivo*.

We are interested in several aspects of p37 palmitylation. The first is to define a motif that specifies palmitylation of VV proteins and perhaps refine it to include all viral and cellular palmitylproteins. Second, we wish to determine the biological function of p37 palmitylation as it pertains to activity of the protein, protein-protein interactions, or targeting to cellular or viral structures. We report here that we have defined a motif specifying palmitylation of p37. Furthermore, palmitylation of p37 is required for correct targeting to intracellular membranes, a prerequisite to function. Our results are discussed within the context of VV biology as well as the general aspects of eukaryotic protein acylation.

EXPERIMENTAL PROCEDURES

Cells and Viruses—BSC_{40} (African green monkey kidney) cells were maintained in Eagle's minimal essential medium (MEM-E) supplemented with 10% (v/v) heat-inactivated fetal calf serum, 2 mM L-glutamine (LG), 10 μg/ml gentamycin sulfate (GS) at 37 °C in a 5% CO_2 humidified atmosphere. The IHD-J strain of VV was routinely propagated and titered in BSC_{40} cells as described previously (26). The mutant virus vRB10 (also referred to as I-VP37) has been described previously (16). It is a derivative of the IHD-J strain in which 93% of the gene encoding p37 has been replaced by the mycophenolic acid resistance gene *gpt* under the control of p7.5K. vRB10 was propagated by low multiplicity passages through BSC_{40} cells in the presence of mycophenolic acid, xanthine, and hypoxanthine. Virus stocks were titered by inoculating serial dilutions onto confluent monolayers of BSC_{40} cells subsequently transfected with plasmid DNA encoding a rescuing copy of the p37 gene (see below). Plaques were visualized by staining infected monolayers with crystal violet 72 h post-infection (HPI).

Computer Analysis of p37—The Net Entrez program was used to find and retrieve the gene and amino acid sequence to p37 from VV strain IHD-J. The sequence was analyzed using the Genetics Computer Group suite of programs to generate a Hopp-Woods (27) hydrophilicity profile and a Chou-Fasman (28) secondary structure prediction. The sequence was then submitted for analysis by TMPred (29)[2] to identify potential transmembrane-spanning regions of the protein.

Construction of p37-encoding Transient Expression Vectors—Plasmid pDG3.0 is a pUC118-based vector that contains the VV *tk* gene into which p7.5K has been inserted. Plasmids pDG4.0, pDG4.1, pDG4.2, and pDG4.3 all have the VV F13L open reading frame cloned adjacent to p7.5K in pDG3.0 such that transcription initiating from p7.5K results in the production of an mRNA that encodes p37. Plasmid pDG4.0 encodes the wild-type p37 protein. Oligonucleotide-directed mutagenesis (30) was used to mutate the F13L sequence in pDG4.0 to generate plasmids pDG4.1, pDG4.2, and pDG4.3. The oligonucleotide oDG4.1 (5′-GCTAACTGGCAGACAAGAAGCTGCAGAGC-3′) was used to construct pDG4.1. It mutates the codon encoding cysteine 185 of p37 to encode serine and introduces a *Pst*I restriction site by silent mutation. Plasmid pDG4.2 was constructed using the oligonucleotide oDG4.2 (5′-GCTAACTGGCAGAGAACAAGCTGCAGAGC-3′). It mutates the codon encoding cysteine 186 of p37 to encode serine and introduces a *Pst*I restriction site by silent mutation. Plasmid pDG4.3 was constructed using oligonucleotide oDG4.3 (5′-GCTCTGCGGCTTCT-TCTCTGCCAGTATGC-3′). The oligonucleotide oDG4.3 mutates the codons encoding cysteines 185 and 186 to encode serine. The mutations were confirmed by DNA sequencing.

Analysis of p37 Modification by Palmitate and Oleate—Subconfluent monolayers of BSC_{40} cells in 35-mm wells were infected with either IHD-J or vRB10 at a multiplicity of infection (m.o.i.) of 10. Concurrent with infection, vRB10-infected cells were transfected with plasmids pDG3.0, pDG4.0, pDG4.1, pDG4.2, or pDG4.3. Liposome-mediated transfection following the method of Rose *et al.* (31) with modifications described by Campbell (32) mediated the transfer of plasmid DNA and transient expression of p37. The inoculum was prepared in polystyrene tubes to which was added 500 μl of MEM-E, the appropriate amount of virus, 30 μl of liposomes, and 10 μg of the appropriate DNA. When no DNAs were to be transfected, liposomes were added to the inoculum as a control. After this mixture remained at room temperature for 15 min, it was added to the cell monolayer from which the culture medium had been aspirated. The cells were placed at 37 °C for 4 h, after which the inoculum was aspirated and replaced with 1 ml of MEM-E with 3% FCS, LG, and GS. At 6 HPI, the culture supernatant was aspirated and the cells washed with warm MEM-E. The wash was aspirated and replaced with 1 ml of MEM-E containing 200 μCi of [9,10-^{3}H]palmitic acid ([^{3}H]PA, DuPont NEN) or 1 ml of MEM-E containing 200 μCi of [9,10-^{3}H]oleic acid ([^{3}H]OA, DuPont NEN). At 24 HPI the cells were harvested in the culture supernatant and transferred to microcentrifuge tubes. The samples were centrifuged at 15,000 × *g* for 30 min to pellet cells and any virions released during the infection. The pellet was resuspended in 60 μl of phosphate-buffered saline (PBS) and freeze-thawed three times. Each cell extract was divided into three fractions of 20 μl each. The first fraction was prepared for immunoprecipitation by addition of 500 μl of a 2 × strength radioimmunoprecipitation assay buffer (1 × RIPA: 1% w/v sodium deoxycholate, 1% v/v Triton X-100, 0.2% w/v SDS, 150 mM sodium chloride, 50 mM Tris-HCl, pH 7.4, and 1 unit/ml Benzonase™ endonuclease) and incubation on ice for 15 min. The samples were then heated to 70 °C for 2 min, followed by centrifugation at 6500 × *g* for 2 min. The supernatant was transferred to new microcentrifuge tubes and the RIPA adjusted to 1 × concentration with water. Anti-p37 antiserum (α-p37) was added to the extracts, followed by incubation on ice for 2 h. 40 μl of a 50% slurry of protein A-Sepharose beads in 1 × RIPA were then added, and incubation was continued for 18 h at 4 °C with constant agitation. The immunoprecipitated proteins were washed three times with 1 × RIPA, transferred to a new microcentrifuge tube, and washed again. The beads were pelleted a final time and resuspended in reducing sample buffer and boiled for 3 min. The proteins were resolved by discontinuous gel electrophoresis (SDS-PAGE), utilizing 12% polyacrylamide gels as described previously (33). Following electrophoresis the gels were fluorographed by impregnation

[2] This program is available on the World Wide Web (http://ulrec3.unil.ch/software/TMPRED_form.html).

with 22.2% PPO in Me_2SO (34), drying, and exposure to Kodak BIOMAX MR film at −70 °C. The second and third fractions from the total cell extracts were directly subjected to SDS-PAGE as described above. One gel was fluorographed as above to detect all vaccinia-encoded [^{3}H]PA- or [^{3}H]OA-labeled proteins. The other gel was subjected to immunoblot analysis (35) by blotting it to a nitrocellulose filter, which was then probed with α-p37. Antigen-antibody complexes on the filter were detected by incubation with goat anti-rabbit antiserum conjugated to alkaline phosphatase (Bio-Rad) and development with 5-bromo-4-chloro-3-indolyl phosphate and *p*-nitro blue tetrazolium chloride.

Plaque Assay—BSC_{40} cells were grown to 95% confluence in 100 mm tissue culture dishes. The cells were infected with IHD-J or vRB10 at high multiplicity (m.o.i. = 10) or low multiplicity (100–300 plaque-forming units/plate). Concurrent to infection with vRB10, the cells were transfected with 300 μl of liposomes and 100 μg of pDG3.0, pDG4.0, or pDG4.3 DNA. Low multiplicity infection/transfections were done in duplicate. The cells were placed at 37 °C for 4 h, after which the inoculum was aspirated and the cells washed once with warm MEM-E. Then 10 ml of MEM-E with 2.5% FCS, LG, and GS were added to each plate, and the cells were placed at 37 °C for the remainder of the experiment. At 24 HPI the cells infected at a high m.o.i. were harvested and assayed for p37 production by SDS-PAGE and immunoblot analysis using α-p37 essentially as described above. Additionally, one set of the duplicate plates infected at a low m.o.i. was stained with crystal violet (0.1% crystal violet in 30% ethanol) at 24 HPI, while the infection of the other set was allowed to continue until 72 HPI. They were then stained with crystal violet as well.

Subcellular Fractionation—BSC_{40} cells were grown to 95% confluence in 100-mm tissue culture dishes. The cells were infected with IHD-J or vRB10 at an m.o.i. of 10. Concurrent to infection with vRB10, the cells were transfected with 300 μl of liposomes and 100 μg of pDG3.0, pDG4.0, or pDG4.3 DNA. The cells were placed at 37 °C for 4 h, after which the inoculum was aspirated and the cells washed once with warm MEM-E. Then, 10 ml of MEM-E with 2.5% FCS, LG, and GS were added to each plate and the cells were placed at 37 °C. In a duplicate experiment, [^{35}S]methionine/cysteine (DuPont NEN) was added to the culture to a final concentration of 25 μCi/ml in the culture supernatant to label nascent peptides. At 12 HPI the culture medium was aspirated and the cells washed free of the plates with 5 ml of ice-cold PBS. The cells were pelleted by centrifugation at 700 × *g* for 10 min, followed by fractionation utilizing differential centrifugation essentially as described by Child and Hruby (22) with modifications as follows. The PBS was aspirated and the cells resuspended in 2.0 ml of hypotonic buffer (HB: 20 mM HEPES, pH 7.6, 5 mM potassium chloride, 1 mM magnesium chloride, 150 mM sodium chloride) and incubated 10 min on ice to swell the cells. All subsequent steps were at 4 °C. The cells were then lysed by Dounce homogenization. One half of the cell lysate (1.0 ml) was set aside as the total cell extract, while the remainder was centrifuged at 700 × *g* for 10 min. The supernatant (post-nuclear supernatant, PNS) was transferred to a new microcentrifuge tube for further fractionation, while the pellet from that centrifugation was resuspended in 1.0 ml of HB and set aside as the nuclear pellet (NP). The PNS was centrifuged at 15,000 × *g* for 30 min. The pellet from this centrifugation was resuspended in 1 ml of HB and set aside as the virus-containing fraction (P15). The supernatant from this centrifugation was transferred to an ultracentrifuge tube and diluted to 4.5 ml with HB and ultracentrifuged at 100,000 × *g* for 60 min. The pellet from this centrifugation was resuspended in 1 ml of HB and set aside as the subcellular organelle/cytosolic aggregate fraction (P100). The supernatant from this centrifugation was adjusted to be 10% trichloracetic acid and centrifuged at 15,000 × *g* for 30 min. The pellet from this centrifugation was set aside as the soluble cytosolic fraction (S100). All other fractions were adjusted to be 10% trichloracetic acid and centrifuged at 15,000 × *g* for 30 min. All precipitated pellets were resuspended in 100 μl of 1 M Tris, pH 10.0, to neutralize the acid and briefly sonicated to facilitate resuspension. Twenty μl of each fraction were analyzed by SDS-PAGE and immunoblot using α-p37 (12% polyacrylamide gel) as well as antiserum directed against the VV major core protein precursor P4a (α-P4a, 10% polyacrylamide gel) and the VV-encoded thymidine kinase (α-TK, 15% polyacrylamide gel). Detection of the rabbit antibody-protein complexes (α-p37, α-P4a, α-TK) was by color development as described above or by chemiluminescence. For chemiluminescent detection, the primary antibody incubation was followed by incubation with goat anti-rabbit IgG horseradish peroxidase conjugate (Pierce). The protein-antibody complexes were detected by incubation with a chemiluminescent peroxidase substrate and exposure to film. Relative quantitation of protein-antibody complexes was performed by film densitometry. To determine the subcellular fractions that contained gp42, cells were infected/transfected as outlined above. The nascent peptides were labeled from 4 until 12 HPI by addition of [^{35}S]methionine/cysteine. At 12 HPI the cells were harvested in PBS and fractionated as described above. Each fraction was subject to immunoprecipitation using a mouse monoclonal antibody to gp42 (α-gp42) essentially as described above. The immunoprecipitated proteins were resolved by SDS-PAGE and fluorographed. The immunoprecipitates were quantitated by film densitometry.

Immunofluorescent Microscopy—BSC_{40} cells were seeded onto microscope slide coverslips ("microcover glasses," VWR) in 35-mm wells at a density of 5 × 10^5 cells/well and cultured at 37 °C for 18 h. They were then infected with either IHD-J or vRB10 at an m.o.i. of 10. The vRB10-infected cells were concurrently transfected with either pDG3.0, pDG4.0, or pDG4.3 as described above. At 12 HPI the culture medium was aspirated and the cells washed once by incubation for 5 min in ice-cold PBS. The wash was aspirated, and the cells were fixed to the microcover glasses by incubation at −20 °C in 100% methanol for 20 min. Immunofluorescent antibody labeling techniques (adapted from Ref. 36) were employed to detect the presence and localization of VV proteins. The cells were washed by two 5-min incubations in ice-cold PBS and then incubated for 2 h at 4 °C in 1 ml of primary antibody solution/well. The antibody solution was prepared as 1:1000 dilutions of either α-p37, α-gp42 or a mixture of α-p37 + α-gp42 in PBS + 5% (v/v) FCS. The primary antibody solution was then aspirated, and the cells washed four times with ice-cold PBS. Five hundred μl of secondary antibody solution were added to each well, and the cells were incubated for 2 h at 4 °C. The cells that had been incubated with the rabbit-produced α-p37 antiserum were incubated with goat anti-rabbit fluorescein isothiocyanate conjugate (GαR-FITC, 1:100 dilution in PBS + 5% FCS, Accurate Chemical & Scientific Corp.) as the secondary antibody. The cells that had been incubated with mouse monoclonal α-gp42 were incubated with goat anti-mouse tetramethylrhodamine isothiocyanate conjugate (GαM-TRITC, 1:200 dilution in PBS + 5% FCS, Accurate Chemical & Scientific Corp.) as the secondary antibody. The cells that had been incubated with the α-p37 + α-gp42 primary antibody mixture were incubated with a secondary antibody mixture of GαR-FITC (1:100 dilution) + GαM-TRITC (1:200 dilution) in PBS + 5% FCS. Following the secondary antibody incubation, the cells were washed four times for 5 min each with ice-cold PBS. After the last wash, the microcover glasses were removed from the tissue culture dishes and allowed to air-dry for 10 min before mounting on microscope slides. Microscopic observations were with a Zeiss photomicroscope through a 10× eyepiece and a 40× oil immersion lens. The rabbit antibody-antigen complexes were visualized by excitation of the FITC fluorophore at 492 nm and observation of fluorescence through a 520-nm filter. The mouse antibody-antigen complexes were visualized by excitation of the TRITC fluorophore at 550 nm and observation of fluorescence through a 570-nm filter. Photographic images were captured on Kodak TMAX 100 black and white film using a Zeiss M35 camera with exposure control by a Zeiss MC 63 on semi-automatic control.

RESULTS

The *in vitro* analysis of p37 by Schmutz *et al.* (25) confirmed the contribution of acylation to the overall biochemical nature of the p37 protein. The protein is very hydrophobic and tightly associated with membranes. Detergent extraction of p37-containing membranes results in p37 partitioning to the detergent-enriched phase normally, but if the extracts are first treated with hydroxylamine, p37 partitions to the aqueous phase. To determine the function of the p37 palmitate moiety *in vivo*, we sought to construct a nonpalmitylating p37 mutant and express it within VV-infected cells and compare its behavior and activity to the wild-type protein.

Computer Analysis of p37—Palmitylation involves the post-translational addition of a 16-carbon saturated fatty acyl moiety via thioester or ester linkage to cysteine, serine, or threonine. Child and Hruby (22) have demonstrated by reverse-phase high performance liquid chromatography that the modifying fatty acid is in fact palmitate and that the palmitate-p37 bond is labile in the presence of hydroxylamine, suggesting that modification occurs through thioester linkage to a cysteine residue. The amino acid sequence of p37 was deduced from the sequence of the VV strain IHD-J F13L gene published by Schmutz *et al.* (37). The protein contains 11 cysteine residues, occurring at amino acid positions 13, 35, 53, 54, 98, 120, 129,

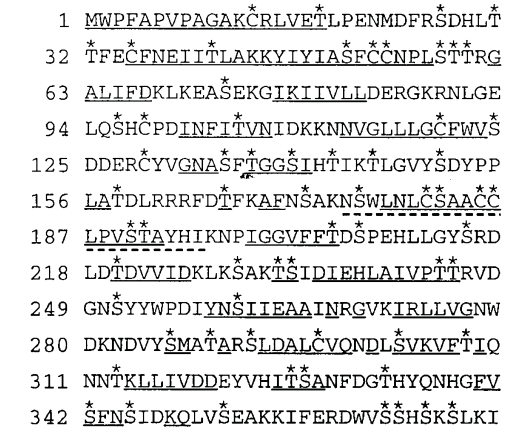

FIG. 1. **Amino acid sequence of p37.** The amino acid sequence of p37 (GenBank™ accession no. 137831 (1991)) is shown using the standard *single-letter amino acid code*. Potential palmitate-acceptor residues (serine, threonine, or cysteine) are indicated by *asterisks* over the residue. Predicted hydrophobic regions are *underlined* with a *solid line*. Predicted transmembrane domains are *underlined* with a *broken line*.

181, 185, 186, and 297 of the 372-amino acid polypeptide. The entire amino acid sequence of p37 was analyzed to predict regions of hydrophobicity, secondary structure, and putative transmembrane regions. Overall, the protein is unremarkable in structure, as predicted by computer-assisted analysis. The central part of the protein contains two major hydrophobic domains, one of which is predicted to be a transmembrane domain as well (Fig. 1). The protein is predicted to consist of 36% α-helices, 30% β-strands/sheets, 21% turns, and the remaining 13% in other structures.

A motif that specifies palmitylation of viral glycoproteins proteins has been previously defined by Ponamaskin and Schmidt (7), but putative identification of the modified cysteine residue(s) could not be made by sequence analysis of p37 alone. However, to facilitate identification of the palmitylation site of p37, we examined numerous palmitylproteins whose site(s) of modification is (are) known in order to potentially refine the reported motif specifying viral glycoprotein palmitylation. Taking into account our analyses of the sequences, secondary structures, and membrane topologies of other palmitylated proteins (data not shown) and previously reported structural requirements for palmitylation, we have arrived at a loosely conserved motif and based our prediction of the palmitylation site(s) of p37 on that. Palmitylation, it seems, occurs most often on cysteine residues 3 to 14 residues downstream (on the cytoplasmic side) of a transmembrane region. The cysteine residue(s) is (are) preceded by two aliphatic residues and is (are) followed by another aliphatic residue. In short, our motif is defined as TMD$X_{1-12}AA$C(C)A, where TMD is transmembrane domain, X is any amino acid, A is any aliphatic amino acid, and C is the palmitylated cysteine(s). On the basis of these criteria, a single region of p37 is predicted to be palmitylated. The cysteine doublet occurring at positions 185 and 186 of p37 is *within* a predicted hydrophobic transmembrane region. The cysteines are preceded by two alanines and followed by a leucine. Although this does not strictly adhere to the structural requirements of the motif, it most closely resembles it. Additionally, the structural requirements defined by Ponamaskin and Schmidt (7) allow for palmitylation of cysteine residues within transmembrane domains but are limited to those occurring within six amino acids from the cytoplasmic border. Cysteines 185 and 186 are located 11 and 10 amino acids away, respectively, from the predicted cytoplasmic border. No other cysteine residues were possible candidates for palmitylation based on our predictions; therefore, we tested this region as the site of palmitylation by site-directed mutagenesis of the cysteine residues predicted to be palmitylated and transient expression of the resulting mutant proteins.

TABLE I
Summary of plasmid constructs

Plasmid	Expression cassette	p37 mutation	PAA[a]	p37+ fractions[b]	p37/gp42 co-localization
pDG3.0	p7.5K:(none)	NA[c]	NA	NA	NA
pDG4.0	p7.5K:F13L	None	++	NP,P15	+
pDG4.1	p7.5K:F13L	C185S	+	ND[d]	ND
pDG4.2	p7.5K:F13L	C186S	+	ND	ND
pDG4.3	p7.5K:F13L	C185S, C186S	–	NP,P15,S100	–

[a] Palmitic acid addition to p37.
[b] Subcellular fractions as described in the text.
[c] NA, not applicable.
[d] ND, not demonstrated.

Identification of the Acylation Site of p37—The recombinant virus, vRB10, a derivative of the IHD-J strain of VV, has had the F13L open reading frame insertionally inactivated and 93% deleted by an exogenous expression cassette mediating antibiotic resistance. This recombinant, although viable in tissue culture, does not produce p37 and consequently does not produce enveloped virions (CEV or EEV) or form plaques on susceptible monolayers of cells as efficiently as the wild-type virus. That these deficiencies were due to the loss of a functional p37 was proven by the restoration of the wild-type phenotype after reinsertion of the F13L open reading frame back into the genome of vRB10 (16). This virus is able to direct the transient expression of proteins provided that the gene encoding them is adjacent to a VV promoter. This is the basis of our analytical system.

We have constructed transient expression vectors that when transfected into VV-infected cells are able to mediate the expression of either the wild-type p37 or mutant forms of p37 containing cysteine to serine permutations at positions predicted to be palmitylated (see Table I). By infection with vRB10, transfection with p37-encoding transient expression vectors, followed by addition of [^{3}H]PA to the cultures, we were able to observe incorporation of label by VV proteins. After harvesting the total cell extracts from infected cells, we first analyzed them for endogenous or transient expression of p37 (Fig. 2*A*) by SDS-PAGE and immunoblot using α-p37. We found that p37 was expressed efficiently from all of our transient expression vectors and from wild-type VV without any p37 being expressed from vRB10. We also analyzed an equivalent fraction of the same extracts for incorporation of labeled palmitate by total VV proteins using SDS-PAGE and fluorography. The profile of palmitylated proteins expressed by vRB10 is identical to IHD-J with p37 being the obvious exception (Fig. 2*C*), although another palmitylprotein of approximately 37 kDa is present. This protein incorporates palmitate less efficiently than p37, but to confirm that it was not p37 from a contaminating source, we then immunoprecipitated labeled p37 from the same total cell extracts and analyzed the immunoprecipitate by SDS-PAGE and fluorography (Fig. 2*B*). No labeled proteins were detected in the immunoprecipitate from vRB10-infected cells. A single protein (p37) was detected in the IHD-J-infected cell extracts as well as the cell extracts in which transient expression of wild-type p37 was mediated by vRB10. Labeled p37 was also detected in vRB10-infected cell extracts where transient expression of p37 was from plasmids pDG4.1 and pDG4.2. The proteins expressed from these plasmids contain mutations that exchange individual cysteines at positions 185 or 186 for serine. Labeled p37 could not be detected in cells that were transfected with pDG4.3, suggesting that the protein expressed from this plasmid is not palmitylated. The protein

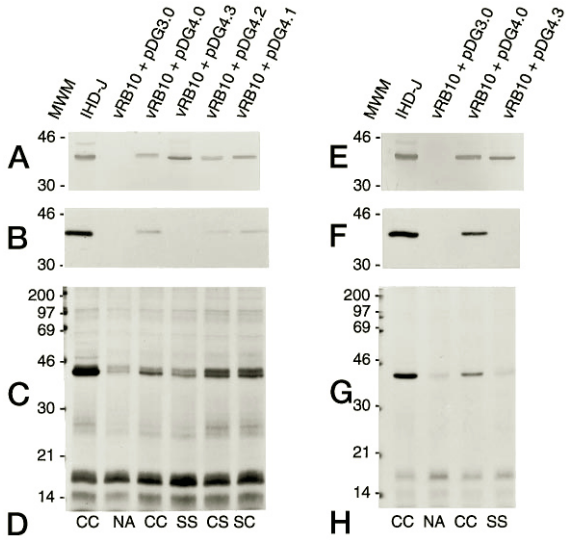

FIG. 2. **Identification of palmitylated cysteine residues.** Cells were infected with either the wild-type IHD-J or the F13L deletion mutant, vRB10. vRB10-infected cells were transfected with the backbone vector (pDG3.0), the wild-type p37 transient expression vector (pDG4.0), or mutant p37 transient expression vectors (pDG4.1, pDG4.2, pDG4.3) as indicated above each gel lane. Tritiated palmitic acid (*A*, *B*, and *C*) or tritiated oleic acid (*E*, *F*, and *G*)) was added to the culture medium after 6 h post-infection. Total cell extracts were harvested at 24 h post-infection. A fraction of the extract was subjected to SDS-PAGE and immunoblot analysis using anti-p37 as the primary antibody (*A* and *E*). An equivalent fraction was subjected to immunoprecipitation by anti-p37 antiserum and then analyzed by SDS-PAGE and fluorography (*B* and *F*). In both panels the only protein detected was p37. A third fraction was directly analyzed by SDS-PAGE and fluorography to detect all VV-encoded palmitylated proteins (*C*) or oleated proteins (*G*). *D* and *H* show the amino acids at positions 185 and 186 of p37. *CC* is wild-type; *CS* contains a cysteine to serine mutation at amino acid 186; *SC* contains a cysteine to serine mutation at amino acid 185; *SS* contains cysteine to serine mutations at amino acids 185 and 186. *NA*, not applicable.

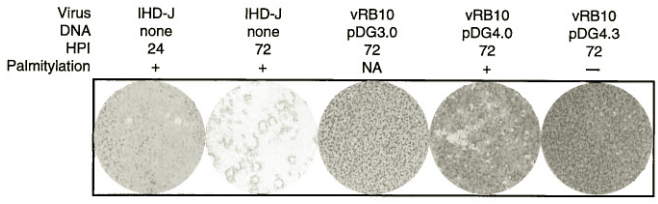

FIG. 3. **Rescue of plaque formation by wild-type and mutant p37.** Monolayers of cells were infected with either the wild-type IHD-J or the F13L deletion mutant, vRB10. Concurrent to vRB10 infection, cells were transfected with either the backbone vector (pDG3.0), the wild-type p37 transient expression vector (pDG4.0), or the nonpalmitylated p37 mutant transient expression vector (pDG4.3). At 24 and 72 HPI, monolayers were stained with crystal violet to allow visualization of plaques.

encoded by pDG4.3 is a mutant that has both cysteines at positions 185 and 186 of p37 replaced by serine. We have concluded that cysteines at position 185 and 186 of p37 are both modified by palmitate and that they are the only sites on the protein that are modified.

Nonpalmitylated p37 Does Not Rescue Plaque Formation by vRB10—Cell-to-cell spread of VV is primarily by EEV and CEV with little contribution from IMV. As a consequence of inactivating the F13L open reading frame, the recombinant virus vRB10 was rendered inefficient at forming plaques on monolayers of cells (16). The process of envelopment and release of virions were efficiently rescued by transient expression or marker transfer of DNA encoding a functional p37. Thus, the ability to rescue plaque formation by vRB10 is an excellent measure of the production of a functional p37 within infected cells. In our experiments, we infected cells with the wild-type IHD-J or vRB10 at high or low m.o.i. Both the high and low m.o.i. infections were concurrently transfected with DNA encoding the wild-type p37 (pDG4.0) or a nonpalmitylating p37 mutant (pDG4.3) under identical conditions. At 24 HPI the cells infected at high m.o.i. were assayed for p37 production by immunoblot analysis using α-p37 as the primary antibody. The protein was expressed in the wild-type IHD-J infected cells and in cells transfected with pDG4.0 or pDG4.3 (data not shown). No p37 was detected in the vRB10-infected cells. Also at 24 HPI, one set of cells infected at low m.o.i. was stained with crystal violet to detect plaques (Fig. 3). IHD-J formed visible plaques at 24 HPI and was just beginning to form the characteristic comet tail-shaped plaques due to the release of EEV. At 24 HPI, no plaques were visible, except by light microscopy, in cell monolayers infected with vRB10 regardless of which DNA was transfected (data not shown). At 72 HPI the second set of identically infected/transfected cells was stained with crystal violet. The IHD-J-infected cell monolayer was completely obliterated, while only very minute plaques were visible in the vRB10-infected cell monolayer. The monolayer of vRB10-infected cells that were transfected with the wild-type p37-expressing vector had plaques equal in size to IHD-J-infected cell monolayers at 24 HPI, with large comet-shaped plaques occurring at an approximate frequency of 1:100 relative to the smaller plaques. The vRB10-infected cell monolayers that were transfected with the vector encoding the nonpalmitylated mutant p37 had only very minute plaques equal in size to those plaques formed in vRB10-infected cell monolayers. No large comet-shaped plaques were observed. By this assay, it seems that a nonpalmitylated p37 is non-functional with regard to envelopment and release of infectious virus, events that are necessary for plaque formation.

The Palmitate Moiety on p37 Mediates Its Membrane Interaction—It has been previously demonstrated that within infected cells, p37 is associated with TGN membranes (15) and that when virion-associated, is found exclusively on the inner face of the EEV outer envelope (25, 38). *In vitro* analysis of the function of the palmitate moiety on p37 suggests that it is the fatty acid that mediates membrane affinity and not the computer-predicted hydrophobic domains in the protein. Schmutz *et al.* (25) performed detergent partitioning studies using normal palmitylated p37 and p37 that had been treated with hydroxylamine to hydrolyze the labile thioester linkage between p37 and the palmitate moiety. The protein was found to partition to the aqueous phase when not palmitylated but was normally found in the detergent phase.

We sought to confirm the *in vitro* findings by an *in vivo* analysis. First we performed differential centrifugation subcellular fractionation of infected cells. Cells were infected with IHD-J or vRB10 at a high m.o.i. The wild-type p37-encoding plasmid or a nonpalmitylating p37 mutant-encoding plasmid were transfected into vRB10-infected cells. At 12 HPI the cells were fractionated as outlined under "Experimental Procedures" to yield a nuclear fraction (NP) and a cytoplasmic fraction (PNS), which was further fractionated into a virus-containing fraction that potentially contains some of the cytoplasmic membrane-bound organelles (P15), a particulate cytoplasmic fraction that has been depleted of virus by the P15 (P100), and a soluble cytoplasmic fraction (S100). We assayed all the fractions for the presence of p37 as well as gp42, the VV major core protein 4a, and the VV-encoded thymidine kinase (TK) as controls. There was no discernible difference between IHD-J-infected cells and vRB10-infected cells as far as the fractionation of 4a and TK were concerned (data not shown). Specifically, the precursor to 4a (P4a) and 4a were found at

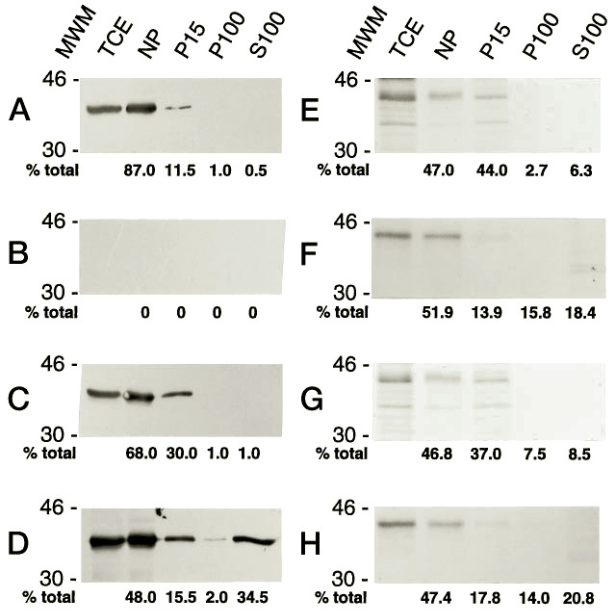

FIG. 4. **Subcellular fractionation of VV-infected cells.** Cells were infected with either the wild-type virus IHD-J (*A* and *E*) or the F13L deletion mutant, vRB10 (*B*, *C*, *D*, *F*, *G*, and *H*). The vRB10-infected cells were transfected with the empty vector pDG3.0 (*B* and *F*), the wild-type p37 transient expression vector pDG4.0 (*C* and *G*), or pDG4.3 (*D* and *H*), a vector transiently expressing a nonpalmitylating p37 mutant. At 12 h post-infection the cells were harvested, lysed, and fractionated by differential centrifugation as outlined under "Experimental Procedures." The resulting fractions were the total cell extract (*TCE*), the nuclear pellet (*NP*), and a cytoplasmic fraction (referred to as the PNS in the text) which was further fractionated into a virus-containing fraction (*P15*), a particulate cytoplasmic fraction (*P100*), and a soluble cytoplasmic fraction (*S100*). In *panels A–D* each fraction was resolved by gel electrophoresis, transferred to nitrocellulose, and sequentially probed with anti-p37 antiserum and goat-anti-rabbit horseradish peroxidase conjugate. Protein-antibody complexes were quantitated by application of chemiluminescent substrate and exposure to film followed by film densitometry. In *panels E–H*, gp42 was immunoprecipitated from ^{35}S-labeled cell extracts fractionated as above. The immunoprecipitate was resolved by gel electrophoresis, fluorographed, and quantitated by film densitometry. The percent of total p37 or gp42 per fraction is given below each gel lane. Each percent is relative to the total detected protein in the NP, P15, P100, and S100 fractions.

approximately the same concentration in the NP as in the PNS. When the PNS was fractionated further, P15 favored 4a over P4a while little of either P4a or 4a was found in the P100. Surprisingly, a significant amount of P4a was found in the soluble cytosolic fraction. Thymidine kinase was found to be present in the PNS and the S100 fractions as would be expected of a soluble enzyme and demonstrates that complete cell lysis has occurred. Within IHD-J-infected cells (Fig. 4*A*), 87% of p37 was present in the NP, 11.5% in the P15, and less than 2% total in the P100 and the S100 fractions. In cells in which the wild-type p37 was transiently expressed (Fig. 4*C*), 68% of p37 was present in the NP, 30% in the P15, and 1% in both the P100 and S100 fractions. The nonpalmitylated p37 (Fig. 4*D*) was present in all fractions. The NP contained 48%, the P15 contained 15.5%, the P100 contained 2%, and the S100 contained 34.5%. Approximately half of the gp42 present in cells was found in the NP regardless of the palmitylation state of p37. When p37 was palmitylated (Fig. 4, *E* and *G*), an approximately equal portion was present in the viral pellet (P15), but when p37 was not present or not palmitylated (Fig. 4, *F* and *H*), gp42 was equally distributed among the P15, P100, and S100 fractions.

The second method to determine the function of the palmitate moiety was by immunofluorescent analysis of infected

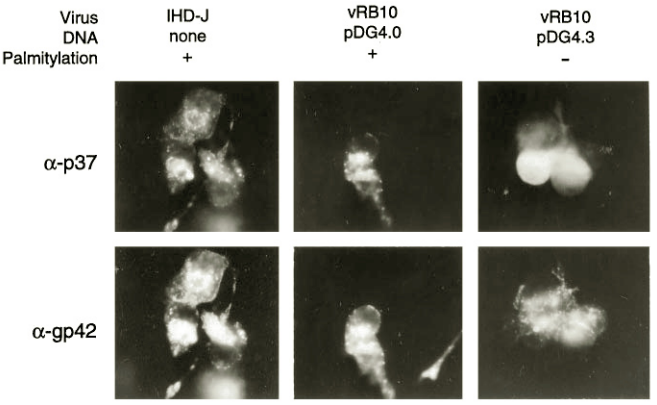

FIG. 5. **Immunofluorescent analysis of p37 localization within VV-infected cells.** Cells were infected with either the wild-type IHD-J or the F13L deletion mutant, vRB10. vRB10-infected cells were transfected with either the wild-type p37 transient expression vector (pDG4.0) or the nonpalmitylated p37 transient expression vector (pDG4.3). At 12 h post-infection the cells were fixed in methanol. The cells were then incubated with rabbit polyclonal anti-p37 and mouse monoclonal anti-gp42 primary antibodies. The secondary antibody incubation included goat-anti-rabbit IgG FITC conjugate and goat-anti-mouse IgG TRITC conjugate. p37-antibody complexes were detected by excitation at 492 nm and observation of fluorescence at 520 nm (α-*p37*). gp42-antibody complexes were detected by excitation at 550 nm and observation of fluorescence at 570 nm (α-*gp42*).

cells. The localization of p37 within infected cells has been previously demonstrated by immunofluorescence (14). When cells have been incubated with fluorescent antibodies directed against p37, a punctate cytosolic pattern of fluorescence is observed, which is indicative of association with cytosolic membrane-bound compartments. We have demonstrated that p37 co-localizes with gp42 (Figs. 4 and 5), another VV-encoded protein that is necessary for envelopment and release of virions. We have observed previously that when this co-localization is disrupted by brefeldin A, no envelopment or egress of virus occurs (39). We therefore sought to determine the intracellular localization of both p37 (wild-type or nonpalmitylated) and gp42 within the same cell as an analysis of correct localization for p37. Cells were infected with IHD-J or vRB10 at a high m.o.i. The vRB10-infected cells mediated the transient expression of wild-type or nonpalmitylated p37 from transfected DNA. The production and localization of p37 and gp42 were demonstrated by indirect immunofluorescence (Fig. 5). The antibody directed against p37 is from polyclonal serum produced in rabbits, while the antibody directed against gp42 is a mouse monoclonal antibody. This allowed us to direct different fluorescent secondary antibodies against the primary antibodies and thus detect the presence of both antigens within the same cell. Within cells infected by IHD-J or vRB10 that were transiently expressing wild-type p37, both p37 and gp42 were present at distinct foci within the cytoplasm of the cell displaying a pattern of fluorescence that was identical for both proteins. At late times after infection (18 and 24 HPI; data not shown), p37 and gp42 were present at the periphery of the cell in addition to cytoplasmic foci. Cells that were expressing the nonpalmitylated p37 displayed a diffuse cytosolic pattern of fluorescence for p37 but gp42-specific fluorescence remained punctate. We have concluded from this observation, as well as from the fractionation studies, that palmitylation not only specifies membrane affinity but that within infected cells targeting to appropriate membranes is abrogated when the palmitate moiety is absent, resulting in solubility in the cytoplasm.

DISCUSSION

In this study, we sought to examine the significance of palmitylation of p37, a major protein constituent of VV EEV enve-

lopes. To facilitate our study, transient expression vectors were constructed in which individual or multiple cysteine residues of p37 were replaced by serine residues. The specific cysteine residues targeted for permutation by serine were predicted to be the palmitate acceptor residues by contextual similarity to the putative palmitylation motif, TMDX_{1-12}*AA*C(C)*A* as described above. The expression of these p37 mutants was mediated by a p37$^-$ mutant VV (vRB10), which allowed analysis of palmitate incorporation and functionality of the protein. Functional analysis included rescue of the non-plaque-forming phenotype of vRB10 as well as experiments to determine the localization of the nonpalmitylating p37 relative to wild-type p37.

Vaccinia Utilizes a Variation of the TMDX_{1-12}AAC(C)A Palmitylation Motif—Not only is p37 the most abundant protein constituent of the EEV envelope, but it appears to quantitatively incorporate more palmitic acid than other palmitylproteins of VV. This suggested to us that the protein may be modified at more than one site. By analysis of numerous palmitylproteins, both viral and cellular, we have defined a motif that we used to predict the palmitylation site of p37. Only one region of the protein was predicted to be palmitylated: a cysteine doublet occurring at positions 185 and 186 of the 372-amino acid polypeptide. Our motif is defined as TMDX_{1-12}*AA*C(C)*A* with the palmitylated cysteine(s) (C) preceded by two aliphatic amino acids (*A*) and followed by another. This occurs most often on residues within or proximal to membrane-spanning domains (TMD). Our motif, as it turns out, is a refinement of one observed for viral glycoproteins (6, 7). Yang *et al.* (40) have observed that the human immunodeficiency virus and simian immunodeficiency virus gp41 protein, a glycosylated, sulfated, transmembrane protein that along with gp120 facilitates CD4 binding, is palmitylated, not proximal to its transmembrane-spanning region, but on cysteines that immediately precede and follow an amphipathic region known to associate with the cytoplasmic face of the plasma membrane. They postulate that palmitylation stabilizes the interaction of the amphipathic region with the membrane. Palmitylation of p37 may serve an analogous function.

Computer analysis predicts two hydrophobic domains in the protein, one possibly being a membrane-spanning region (Fig. 1). Considering the data presented in this study and the work of Schmutz *et al.* (25), it seems unlikely that p37 spans the membrane of the TGN or virion envelopes, even though it is tightly associated with them. Releasing p37 from the membrane requires only treatment with hydroxylamine, which cleaves the thioester palmitate-cysteine linkage. Additionally, the nonpalmitylating mutant described here is found to fractionate with the soluble cytoplasmic components of infected cells, as well as displaying a diffuse cytosolic pattern when examined by immunofluorescent microscopy. Our *in vivo* work confirms the *in vitro* analysis of p37. We have concluded that the membrane affinity of p37 is in large part mediated by palmitylation of cysteine residues at positions 185 and 186 of the polypeptide chain.

Our motif, as it seems, is imperfect and will require refinement in order to accurately predict the palmitylation sites of non-transmembrane-spanning proteins. Nevertheless, we were able to predict the palmitylation site of p37 based on the motif. When either cysteine 185 or cysteine 186 was replaced by serine, we observed a reduction in the efficiency of [3H]PA incorporation by p37 (Fig. 2*B*). The immunoblots of the same infected cell extracts (Fig. 2*A*) indicate that similar amount of protein were expressed relative to the transiently expressed wild-type protein, but the absolute efficiency of palmitylation at either cysteine residue was not measured.

In addition to modification by palmitate, p37 is subject to oleation (41). When VV-infected cells were cultured in the presence of [^{3}H]OA and total cell extracts were analyzed by SDS-PAGE and fluorography, we observed incorporation of label by proteins with apparent masses of 14, 17, 23–28, 37 (p37 and an additional co-migrating 37-kDa oleated protein), 41, 56, 86, and 92 kDa (Fig. 2*G*). All of these proteins appear to co-migrate with known palmitylproteins of VV, suggesting that VV palmitylproteins belong to the class of "*S*-acylated" proteins that are preferentially palmitylated but alternatively are subject to modification by other long-chain fatty acids (reviewed in Refs. 6 and 42). To be certain that oleation of p37 did not occur at a site different than the palmitate acceptor site, we transiently expressed the nonpalmitylating p37 mutant in vRB10-infected cells in the presence of [^{3}H]OA and assayed for incorporation of label by p37. Although the protein could be detected by immunoblot (Fig. 2*E*), it could not be detected by fluorography (Fig. 2*F*), suggesting that the protein was not modified by oleate if the palmitate acceptor cysteines were substituted with serine as would be expected for a *S*-acylated protein.

Palmitylation of p37 Is Required for Correct Localization and Function—Enveloped virus, specifically CEV and EEV, are responsible for cell-to-cell spread of VV and consequently plaque formation on susceptible monolayers of cells. The requirement of p37 in this process has been previously established (43). When we transiently expressed wild-type p37 in vRB10-infected cells, plaques were formed, albeit at a slower rate than for IHD-J. We initially attributed this to one of two possibilities: (i) plasmid-mediated expression did not provide the correct context for function, or (ii) expression kinetics from p7.5K were sufficiently different from the F13L endogenous promoter that normally synchronous events were perturbed. Examination of infected cells by immunofluorescent microscopy suggested a third explanation. Transfection efficiency, as determined by the ratio of cells fluorescently labeled by α-p37/GαR-FITC, ranged from 10 to 50% depending on which preparation of liposomes was used to mediate the transfection. It stands to reason that cell-to-cell spread would be inefficient under those conditions. On the other hand, cell-to-cell spread by vRB10, when the only rescuing copy of p37 was not palmitylated, was even less efficient. Throughout the course of the experiment, the efficiency of plaque formation never exceeded that observed for vRB10 when p37 is not palmitylated. One other phenotype that we observed when the rescuing copy of p37 was wild-type, was the formation of large comet-shaped plaques occurring at an approximate frequency of 1:100 relative to the smaller plaques. We assume that this is due to recombination between the plasmid copy of the F13L gene and the VV genome, which contains intact 5′ and 3′ sequences of F13L. Cell-to-cell spread would be much more efficient if the virus expressed p37 from its genome instead of relying on the plasmid copy of the gene, which is present in only 10–50% of the cells. When the nonpalmitylating p37 is expressed in vRB10-infected cells, all plaques formed were uniform in size. Considering that recombination frequency appears to be about 1 in 100, there does not seem to be any selective advantage for recombinants that are expressing the nonpalmitylating p37 from their genomes. Further analysis of the significance of p37 palmitylation may require the isolation of recombinants that express the nonpalmitylating p37 mutant. This may prove to be difficult considering the lack of selection for recombinants and the pressure to mutate back to wild-type once recombined.

We have considered the possibility that enveloped virions are formed and released but are not infectious. We have taken two approaches to address this possibility. First we attempted to purify virions from IHD-J- and vRB10-infected cells trans-

fected with either wild-type or nonpalmitylated p37-encoding plasmids. We were able to demonstrate that IHD-J produced both IMV and EEV by CsCl gradients (data not shown) since they are separable by characteristic densities. While vRB10-infected cells produced normal amounts of IMV, the production of EEV could not be demonstrated even when a rescuing wild-type copy of p37 was expressed in those cells. We then attempted to assay for EEV-specific proteins in the infected cell culture supernatants. This proved to be even less sensitive, as we were unable to demonstrate conclusively, the presence of gp42 (data not shown) in IHD-J-infected cell culture supernatants. To address the possibility of noninfectious EEV release will probably require the construction of recombinant VV that expresses the nonpalmitylated p37, and, as alluded to above, this may prove difficult.

As to why the nonpalmitylating p37 mutant is not functional, we considered three possibilities. (i) Palmitylation of proteins has been demonstrated to activate a protein, usually by targeting the protein to a site where it serves its function (1). The protein is then inactivated by depalmitylation, resulting in diffusion away from the site of function. (ii) Palmitylation can mediate protein-protein interactions (2). (iii) Alternatively, as is most often the case, palmitylation mediates protein-membrane interaction (2). We do not consider palmitylation of p37 to be an activation switch. All of the p37 within a cell appears to localize to its site of function, specifically, intracellular membranes (Figs. 4, *A* and *C*, and 5), and by this study we know that interaction to be dependent on palmitylation of p37. The lack of any detectable (wild-type) p37 in the soluble cytoplasmic fraction of cells argues against regulation of p37 by reversible palmitylation.

There are reports that claim p37 covalently interacts with gp42 (41) and possibly noncovalently with the viral hemagglutinin (44). Recent work by Schmutz *et al.* (25) argues against either interaction. Within infected cells, p37 exists solely as a monomer, and in purified virions it exists as a monomer and a homodimer. The latter represents the minority of the total p37 present in EEV membranes, and its significance is not known. Considering that homodimerization occurs after envelopment and that the nonpalmitylating p37 mutant cannot mediate the envelopment and release of virions, it seems unlikely that the loss of function is due to the inability of p37 to dimerize.

This leaves membrane targeting/anchoring as the remaining possible function for palmitylation of p37. The work by Schmutz *et al.* (25) suggested as much *in vitro*, and our *in vivo* analysis confirms it. When VV-infected cells are fractionated by differential centrifugation, we find that wild-type p37 is concentrated in the particulate membrane-containing fractions (Fig. 4, *A* and *C*) in agreement with previously published reports (22). When p37 is not palmitylated, it is found in the membrane-containing fractions as well as the soluble cytosolic fractions (Fig. 4*D*). If the subcellular fractionation results are analyzed independent of the rest of this study, one might conclude that the palmitate moiety only serves to anchor p37 in a membrane that it has an intrinsic affinity for. This is a reasonable assumption but one that is not supported by immunofluorescent analysis of infected cells. Prior to virion association, p37 localizes to the TGN and by immunofluorescent analysis appears to co-localize with gp42 (Fig. 5) in agreement with immunoelectron microscopy work performed by Schmelz *et al.* (15). Indirectly labeling p37 or gp42 via fluorescently tagged antibodies results in identical punctate cytosolic foci of fluorescence within infected cells. If palmitylation of p37 served only to anchor the protein to its target membrane, one would expect that the nonpalmitylating p37 mutant would continue to co-localize with gp42 with little diffusion away from those sites. In fact, the opposite is true. The nonpalmitylating p37 mutant exhibits a diffuse cytosolic pattern of fluorescence with no discrete foci anywhere within infected cells. The pattern of fluorescence for gp42 remains undisturbed in cells expressing the nonpalmitylating p37 mutant, and, as such, p37 must not be involved in gp42 targeting to membranes. It is possible, though, that gp42 is involved in p37 targeting through interaction with its palmitate moiety as has been described for other protein-protein interactions (2).

Why though does most of the wild-type p37, and a significant portion of the nonpalmitylated p37, fractionate with the particulate fractions of the cell when it is thought to only associate with the TGN when palmitylated and remain soluble when palmitylation is blocked? Perhaps the lysis conditions favor aggregation in macromolecular structures, a possibility we have not investigated. It is also conceivable that the VV-induced reorganization of cytoskeletal structure (45) may alter the fractionation of subcellular components relative to uninfected cells. Nevertheless, a significant portion of the nonpalmitylated p37 found in the cytoplasmic fraction of infected cells is soluble and, when observed by immunofluorescence, displays a fluorescent pattern one would expect from a soluble cytoplasmic protein.

Vaccinia virus continues to stand out as a uniquely capable model system for the analysis of eukaryotic protein processing. In addition to acylation, VV polypeptides are subject to proteolytic processing, glycosylation, phosphorylation, ADP-ribosylation, disulfide cross-linking (reviewed in Ref. 46), and sulfation (41). We have yet to decipher all the intricacies of these modifications in VV or eukaryotic systems, and palmitylation of proteins is one of the least understood of these processes. Perhaps exploitation of the VV system will allow us to not only accurately predict protein palmitylation but identify factors mediating the process, including those responsible for the modification reaction and molecular properties of the modified protein.

Acknowledgments—We thank Dr. Bernard Moss for providing vRB10. We are also grateful to Dr. Lendon Payne and Dr. Riccardo Wittek for providing antisera to gp42 and p37, respectively.

REFERENCES

1. Shenoy-Scaria, A. M., Dietzen, D. J., Kwong, J., Link, D. C., and Lublin, D. M. (1994) *J. Cell Biol.* **126,** 353–363
2. Wedegaertner, P. B., Wilson, P. T., and Bourne, H. R. (1995) *J. Biol. Chem.* **270,** 503–506
3. Hruby, D. E., and Franke, C. A. (1993) *Trends Microbiol.* **1,** 20–25
4. Bizzozero, O. A., Tetzloff, S. U., and Bharadwaj, M. (1994) *Neurochem. Res.* **19,** 923–933
5. Magee, A. I., and Courtneidge, S. A. (1985) *EMBO J.* **4,** 1137–1144
6. Schmidt, M. F. G. (1989) *Biochim. Biophys. Acta* **988,** 411–426
7. Ponamaskin, E., and Schmidt, M. F. G. (1995) *Biochem. Soc. Trans.* **23,** 565–571
8. Zurcher, T., Luo, G., and Palese, P. (1994) *J. Virol.* **68,** 5748–5754
9. Jin, H., Subbarao, K., Bagai, S., Leser, G. P., Murphy, B. R., and Lamb, R. A. (1996) *J. Virol.* **70,** 1406–1414
10. Dietzen, D. J., Hastings, W. R., and Lublin, D. M. (1995) *J. Biol. Chem.* **270,** 6838–6842
11. Moss, B. (1990) in *Virology* (Fields, B. N., Knipe, D. M., Chanock, R. M., Hirsch, M. S., Melnick, J., Monath, T. P., and Roizman, B., eds) pp. 2079–2111, Raven Press, New York
12. Goebel, S. J., Johnson, G. P., Perkus, M. E., Davis, S. W., Winslow, J. P., and Paoletti, E. (1990) *Virology* **179,** 247–66, 517–563
13. Sodeik, B., Doms, R. W., Ericsson, M., Hiller, G., Machamer, C. E., van't Hof, W., van Meer, G., Moss, B., and Griffiths, G. (1993) *J. Cell. Biol.* **121,** 521–542
14. Hiller, G., and Weber, K. (1985) *J. Virol.* **55,** 651–659
15. Schmelz, M., Sodeik, B., Ericsson, M., Wolffe, E. J., Shida, H., Hiller, G., and Griffiths, G. (1994) *J. Virol.* **68,** 130–147
16. Blasco, R., and Moss, B. (1991) *J. Virol.* **65,** 5910–5920
17. Engelstad, M., and Smith, G. L. (1993) *Virology* **194,** 627–637
18. Isaacs, S. N., Wolffe, E. J., Payne, L. G., and Moss, B. (1992) *J. Virol.* **66,** 7217–7224
19. Rodriguez, J. F., and Smith, G. L. (1990) *Nucleic Acids Res.* **18,** 5347–5351
20. Parkinson, J. E., and Smith, G. L. (1994) *Virology* **204,** 376–390
21. Ravanello, M. P., and Hruby, D. E. (1994) *J. Gen. Virol.* **75,** 1479–1483
22. Child, S. J., and Hruby, D. E. (1992) *Virology* **191,** 262–271
23. Duncan, S. A., and Smith, G. L. (1992) *J. Virol.* **66,** 1610–1621

24. Hirt, P., Hiller, G., and Wittek, R. (1986) *J. Virol.* **58,** 757–764
25. Schmutz, C., Rindisbacher, L., Galmiche, M. C., and Wittek, R. (1995) *Virology* **213,** 19–27
26. Hruby, D. E., Guarino, L. A., and Kates, J. R. (1979) *J. Virol.* **29,** 705–715
27. Hopp, T. P., and Woods, K. R. (1981) *Proc. Natl. Acad. Sci. U. S. A.* **78,** 3824–3828
28. Chou, P. Y.,and Fasman, G. D. (1978) *Annu. Rev. Biochem.* **47,** 251–276
29. Hofmann, K., and Stoffel, W. (1993) *Biol. Chem. Hoppe-Seyler* **347,** 166
30. Kunkel, T. A., Roberts, J. D., and Zakour, R. A. (1987) *Methods Enzymol.* **154,** 367–382
31. Rose, J. K., Buonocore, L., and Whitt, M. A. (1991) *Biotechniques* **10,** 520–525
32. Campbell, M. J. (1995) *Biotechniques* **18,** 1027–1032
33. Studier, F. W. (1973) *J. Mol. Biol.* **79,** 237–248
34. Bonner, W. M., and Laskey, R. A. (1974) *Eur. J. Biochem.* **46,** 83–91
35. Towbin, H., Staehelin, T., and Gordon, J. (1979) *Proc. Natl. Acad. Sci. U. S. A.* **76,** 4350–4354
36. Watkins, S. (1991) in *Current Protocols in Molecular Biology* (Ausubel, F. M., Brent, R., Kingston, R. E., Moore, D. D., Seidman, J. G., Smith, J. A., and Struhl, K., eds) CD-ROM Edition, Unit 14.6, Greene/Wiley Interscience, New York
37. Schmutz, C., Payne, L. G., Gubser, J., and Wittek, R. (1991) *J. Virol.* **65,** 3435–3442
38. Payne, L. (1978) *J. Virol.* **27,** 28–37
39. Ulaeto, D., Grosenbach, D., and Hruby, D. E. (1994) *J. Gen. Virol.* **76,** 103–111
40. Yang, C., Spies, C. P., and Compans, R. W. (1995) *Proc. Natl. Acad. Sci. U. S. A.* **92,** 9871–9875
41. Payne, L. (1992) *Virology* **187,** 251–260
42. Casey, P. J. (1995) *Science* **268,** 221–225
43. Blasco, R., and Moss, B. (1992) *J. Virol.* **66,** 4170–4179
44. Oie, M., Shida, H., and Ichihashi, Y. (1990) *Virology* **176,** 494–504
45. Cudmore, S., Cossart, P., Griffiths, G., and Way, M. (1995) *Nature* **378,** 636–638
46. VanSlyke, J., and Hruby, D. E. (1990) *Curr. Top. Microbiol. Immunol.* **163,** 185–206